Kalt, Peter Anthony Markus; Dally, Bassam The effect of jet preheating on turbulence in a premixed jet in hot coflow Proceedings of the Australian Combustion Symposium, Perth, WA, 6-8 November 2013 / Mingming Zhu, Yu Ma, Yun Yu, Hari Vuthaluru, Zhezi Zhang and Dongke Zhang (eds.): pp.255-258

Proceedings of the Australian Combustion Symposium
November 6-8, 2013, The University of Western Australia

The Effect of Jet Preheating on Turbulence in a Premixed Jet in Hot Coflow

P.A.M. Kalt[1,*] and B.B. Dally[1]
[1]Centre for Energy Technology
University of Adelaide SA 5005 Australia

Abstract

Moderate or Intense Low oxygen Dilution (MILD) combustion is an important combustion regime, which utilises the combustion of gas in hot and often vitiated environment. MILD combustors are characterised by the use of exhaust gases recirculated into the combustor via dilution or mixing with the incoming fuel or alternately by rapidly mixing an incoming fuel stream into a hot environment of combustion products. However, the influence of preheating the fuel jet is not well understood. Current approaches rely heavily on assumptions about the role of heat on laminarisation of turbulence, due to viscosity. However, the density ratio between jet and environment is known to have a dominant effect on mixing. Velocity measurements are presented for a pair of turbulent premixed flames issuing into a premixed coflow. Two cases are considered, both with and without preheating of the central fuel jet. The resulting near-field velocity is measured using digital Particle Image Velocimetry (PIV). The resulting velocity maps are processed to find the turbulence intensity, u'/U. A two-point correlation technique is used to determine the turbulence integral length scale, l_f. The influence of preheating the central jet on the resulting near-field turbulence characteristics are presented and discussed.

Keywords: MILD combustion, Integral Lengthscales, Turbulence Intensity, Particle Image Velocimetry.

1. Introduction

1.1 MILD Combustion

Moderate or Intense Low-oxygen Dilution (MILD) combustion has attracted the attention of many researchers due to the many attractive features in reducing emission and improving thermal efficiency. This combustion mode relies on heat and gas recirculation to establish a distributed reaction zone with a semi-uniform furnace temperature above that of autoigniton, usually above 800 ℃ [1,2,3]. Design of new and adaptation of old burners to work under these conditions requires further research to ensure effective mixing and reaction of the reactants under these conditions. In the majority, fuel jets are injected into a hot medium of products and oxidant at lower density [4,5,6]. Much documented research points to delay ignition, preheating of the premixing of the fuel before reaction can proceed [6]. The impact of this preheating on the mixing and reaction is of interest to this study.

Many researchers have investigated variable density jets and the impact they have on the mixing, spread and decay of the jets [7-12]. Fewer have investigated the influence of heat release due to combustion reactions of such jets [13-15]. Some of the major findings out of these studies can be summarized as follows:

- The rates of spread and decay of a simple jet issuing into a higher density fluid is more rapid than that issuing into a lighter fluid with either the same momentum flux or the same Reynold's number [10].
- Reynolds number plays an important role in determining the turbulent structure, centerline unmixedness and virtual origin location for variable density jets [7,8,9,11].
- Heat release (i.e flame) suppresses or laminarizes the turbulence especially in the outer layer of the jet where the gas temperature is high leading to the increase in kinematic viscosity and the retardation of mixing. And while non-reacting cold jets have high centerline turbulence closer to the jet exit, flames promote turbulence farther downstream because of the higher velocity gradient due to the expansion by the temperature rise [13,14].
- The reaction zone appears to act as a boundary condition for a shear layer that is formed between the high-speed jet fluid and the combustion products from the reaction zone. The lower density ratio under reacting conditions reduces the growth rate of the near field shear layer, thus extending the potential core of the jet [15].
- The position of the stoichiometric mixture fraction relative to the shear layer have less impact on the mixing as compared to the density ratio [15]
- RANS based models seem to be inconsistent in predicting the spread and decay of a cold jet in a hot coflow over a moderate span of Reynolds number [16].

In this paper we investigate the impact of preheating a premixed CH_4/Air jet issuing into a hot and diluted environment on the flow field and its turbulence characteristic.

2. Experimental

2.1 Jet in Hot-Coflow Burner

For this study the Jet in Hot Coflow burner (JHC) was used to stabilise two premixed flames in a vitiated coflow under MILD conditions. The JHC burner [17] is shown in Fig. 1. In this study the central jet diameter was 15 mm. Turbulence was generated within the

* Corresponding author:
Phone: (+61) 8 83132304
Email: peter.kalt@adelaide.edu.au

central jet by means of an upstream perforated plate (0.8mm holes on a 1.5mm pitch, blockage 74%). The burner was located in a shrouded enclosure to assist in the extraction of combustion products and to isolate the burner from the effects of the surrounds (ambient velocity <0.1m/s).

The flames investigated here comprised lean premixed CNG/ethylene/Air jets issuing into a premixed CNG/ethylene/Air coflow. This fuel mixture is analogous to pure methane. Compressed natural gas was sweetened with 1% ethylene (by volume) so that the flame speed of the CNG mixture (as reported by the supplier) matched that of pure methane for the same stoichiometry. The difference between CNG and methane is often ignored, however for these lean flames, the stability limits for the burner are very sensitive to fuel variation.

Both flames studied here had the same stoichiometry in the central jet and coflow. The equivalence ratio of both the central jet and surrounding coflow was 0.7. The primary difference between investigated cases was that the central jet was preheated in one case (T_{jet} = 650K), and not in the other (T_{jet} = 300K), in order to observe the effect of preheating common to MILD applications. The mass flow rates of both flames are the same, however the **heated jet** case will have higher velocities than the **cold jet** due to thermal expansion of the jet gases. Jet flow rate is 270 slm, and coflow is 163 slm, although the volume rate will depend on the temperature of the gases.

Preheating the jet gases was performed using a high-flow rate gas heater drawing 3-phase power. Given the mass flow through the heater, the maximum temperature that could be consistently gained was 350 ^{o} above ambient. This jet temperature was measured at the exit plane using a K-type thermocouple.

2.2 Imaging and Lasers

Velocity was measured using a cross correlation digital PIV technique, conducted in the TEC Laboratory at the University of Adelaide, shown schematically in Fig. 2. Illumination is provided by a Quantel Brilliant-B double pulsed Nd:YAG laser using the second harmonic at 532nm. Laser power was comparatively low (~100mJ/pulse) given the imaging region and the general efficiency of Mie-scattering. The time delay between successive laser pulses was 100 μs.

The imaging system comprised a Megaplus II 2093 camera running in triggered double exposure mode at 2.5Hz. Collection optics were a Tamron 80-200 compound lens imaging a region of 184 mm by 104 mm onto the detector of 1920 pixels by 1080 pixels. Magnification is therefore 13:1, with 10.4 pixels per mm. The imaging system comprised a Megaplus II 2093 camera running in triggered double exposure mode at 2.5Hz. Collection optics were a Tamron 80-200 compound lens imaging a region of 184 mm by 104 mm onto the detector of 1920 pixels by 1080 pixels. Magnification is therefore 13:1, with 10.4 pixels

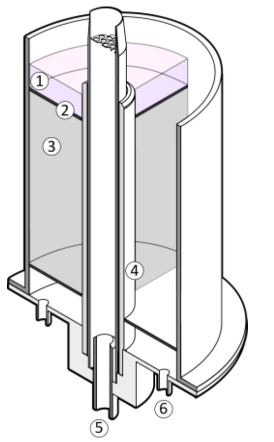

Figure 1: Schematic of the Jet in Hot Coflow (JHC) burner.

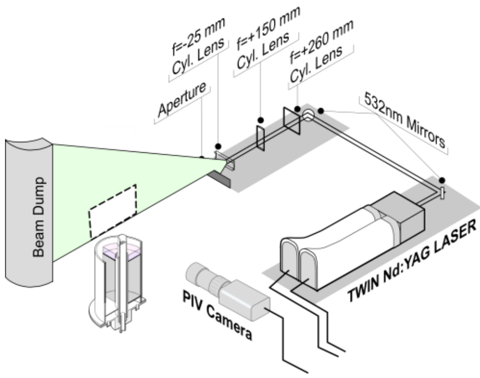

Figure 2: Schematic of the imaging system used for digital Particle Image Velocimetry (PIV).

per mm. Given a PIV interrogation window of 32 pixels by 32 pixels, this relates to an in plane resolution of approximately 3 mm. Given that the laser sheet is formed with a thickness of 2 mm, the in-plane resolution is the limiting factor.

The resulting Mie-scattering image pairs were processed using PIVView software. Careful attention was paid to the processing parameters to ensure that the velocity field was not conditioned artificially. The final cross-correlation was performed on an interrogation window of 32 by 32 pixels. However, the final correlation sub-region was offset by a displacement determined by grid refinement, in 5 steps from 256 pixels. Gaussian peak fitting was selected to avoid peak locking effects and give sub pixel accuracy on determined displacements.

No filtering or smoothing was applied to the resulting vector field as this broadens any derived 2-pt correlations by 'leaking' the value of one vector into its neighbours. Outlying vectors were crudely evaluated as any vector more than 3 times the local average. Such vectors were replaced by a distance-weighted average of neighbours. However, in the region of interest the PIV processing was extremely strong and outliers were negligible. The PIV ensemble consisted of 300 image pairs.

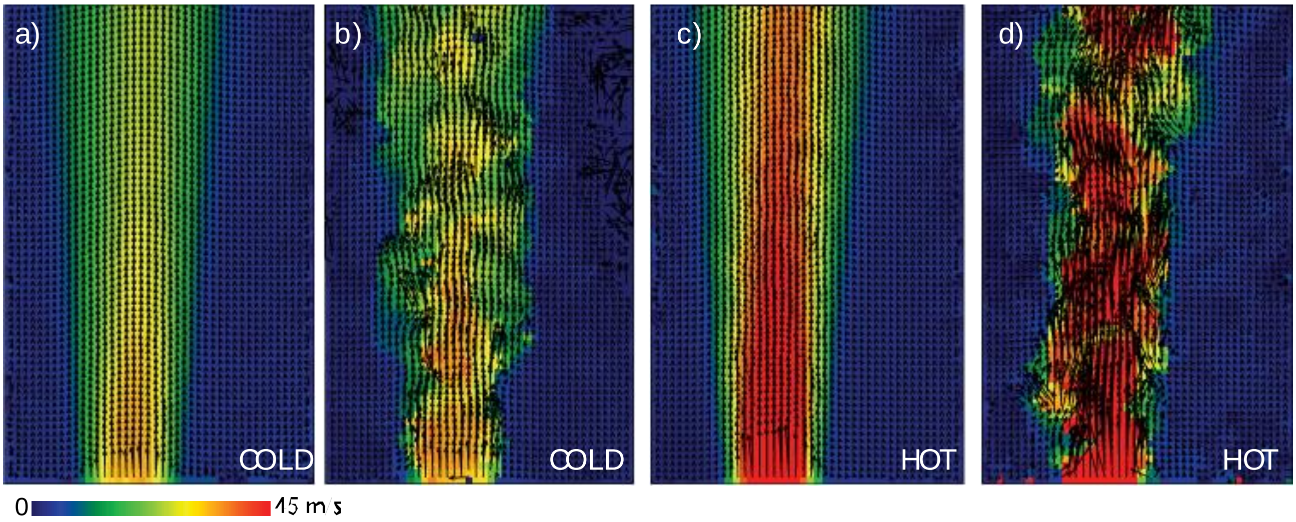

Figure 3: a) b) Mean and instantaneous velocity fields for unheated jet flame; c) d) mean and instantaneous velocity fields for heated jet flame.

2.3 Two-Point Correlation and Fitting

Each ensemble of 300 vector images was used to determine a two-point velocity correlation for the purpose of determining the integral lengthscale of turbulence, using the method of Chen *et al.* [18].

To determine the two-point correlation, a location of interest must be determined. For this experiment a point on the burner centerline and 30 mm downstream of the burner exit is selected. Such a location is always in the vitiated coflow region and is representative of a MILD combustion environment. Locations that are further downstream may run the risk of showing the influence of entrained surroundings.

The two-point longitudinal correlation functions of the axial velocity component at position (x,r) are calculated with Eq. 1 from 300 processed instantaneous PIV velocity fields.

$$f(\Delta x) = \frac{\overline{u'(x,r)u'(x+\Delta x,r)}}{[\overline{u'(x,r)^2}]^{1/2}[\overline{u'(x+\Delta x,r)}]^{1/2}} \quad (1)$$

where Δx is the axial distance between two velocity vectors at the same radius, r. In order to test the variability of the two-point correlation, the lengthscale is also determined using several neighbouring locations adjacent to the centerline reference point.

Longitudinal integral lengthscale, l_f, is derived by curve-fitting $f(\Delta x)$ with Eq. 2 [18].

$$f(\Delta x) = a\left(1 - \frac{b\Delta x}{2}\right)e^{-b\Delta x} + c\left(1 - \frac{d\Delta x}{2}\right)e^{-d\Delta x} \quad (2)$$

Thus, l_f is calculated as $a/2b + c/2d$. Application of the curve-fit is done here using a Monte-Carlo method using at least 10^6 iterations until the *chi* value is typically less than 0.05. As a guide to interpreting the correlation decay and curve fits (Fig. 5 a) and b)), the integral lengthscale approximately corresponds to the number of vector increments required for the correlation to decay to 50%.

3. Results and Discussion

Figure 3 shows a pair of velocity fields from the two flame cases studied here. Figures 3a) and c) show the mean velocity fields for the cold and hot jets, respectively. The average vector fields are superimposed on a false-colour image indicating the axial component of velocity. Interestingly, the spread of the jet appears to be the same for both cases. Figures 3b) and d) show typical instantaneous velocity fields for the cold and hot jet cases, respectively. The large-scale turbulence structures within both jets, revealed by spatial variations in the false-colour image appear broadly similar. In fact, the clearest difference between the cold and hot jets is that the heated jet case has much higher average velocity, but is otherwise macroscopically similar.

Figure 4 shows the centerline velocity decay for the two jets. The axial component of velocity on the centerline is plotted, normalized by the maximum centerline value, U/U_{max}. The spatial coordinate (x-axis) is the downstream distance normalized by the jet diameter, x/D. The heated jet case, shown using the hollow diamond symbols, decays slightly faster than the cold jet case, plotted with solid square symbols. Both jets show the expected peak of axial velocity not at the burner exit but in the potential core approximately one diameter after the burner exit. The increased rate of decay for the hot jet, without broader spreading, can be attributed to a laminarisation effect due to elevated temperatures increasing the viscosity of the heated jet fluid.

Figure 5 shows the 2-point correlation coefficient for the a) cold and b) hot jets taken at the centerline reference positions, located 30 mm downstream of the burner exit. The curve-fits to the raw two-point correlation data are also shown in the figures. It is most important for the curve fit to focus on correctly capturing the initial decay in the correlation. At downstream locations the correlations should decay to zero if the far field is uncorrelated with the turbulence in the potential core. Non zero values for the two-point correlation in this region indicate that there is some large scale puffing or flapping that is being seen in the correlation. This could correspond to the largest scales of coherent structures that can be seen in Figs. 3b) and d). The heated jet shows more large scale flapping motions at far downstream. This is likely to result from the higher jet velocity in this case, extending the

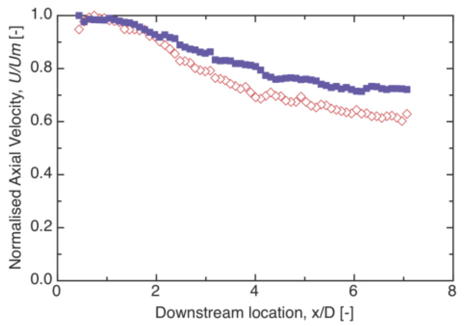

Figure 4: Plots showing the decay of normalized axial velocity for the hot (hollow diamond) and cold (solid square) conditions.

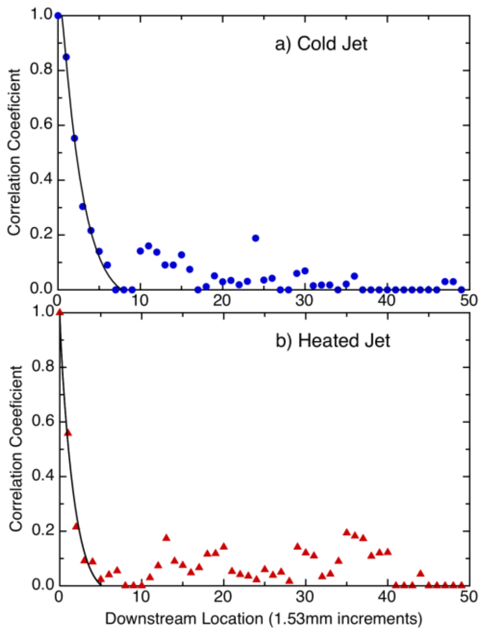

Figure 5: Correlation Coefficients and lengthscale curve fit for: a) unheated jet; and b) heated jet, at the centerline reference position.

potential core of the jet and pushing it out of the region dominated by the hot coflow. However, the more noteworthy difference is in how the correlation decays close to the reference position, noticeably faster in the heated jet than the cold jet case.

Figure 6 plots the determined lengthscale against the turbulence intensity, u'/U. Several interesting observations can be drawn from this graph. Firstly, it is clear that the role of preheating the central jet serves to reduce the lengthscale. This would indicate an *increase* in grid-induced turbulence for the heated jet case, since the turbulence is expected to start at the grid size (0.8mm) and grow as it decays. Additionally, the turbulence intensity is also higher at 20-25% of the bulk velocity.

4. Conclusion

In summary the role of jet preheating on the turbulence characteristics of a premixed jet is not straightforward. It seems that there are competing effects: one towards laminarisation due to thermal viscous effects; the other an increase in velocity and kinetic energy due to thermal expansion. Increasing velocity can have a dominant effect in geometries that exploit grid-induced turbulence, or use the jet flow to induce mixing. However, jet momentum flux (twice as

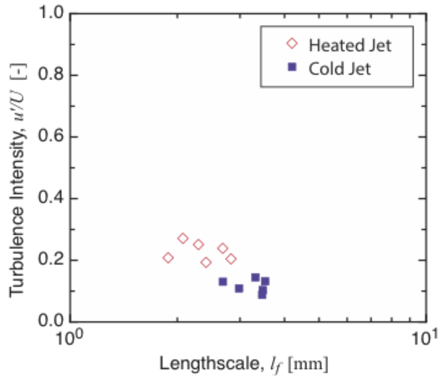

Figure 6: Turbulence intensity, u'/U, vs integral lengthscale, l_f.

fast, half as dense) does not change significantly and this is confirmed by the similarity in normalized mean images of the jet spread (Fig. 3).

Further work is needed to completely identify the competing roles of thermal laminarisation and expansion-induced turbulence. However, a lengthscale decrease from 3.2mm to 2.3mm (27%) is expected to have a significant role on the flames characterization within a premixed combustion regime.

5. Acknowledgments

This work was made possible using equipment at the Centre for Energy Technology at the University of Adelaide.

6. References

[1] Tsuji H, Morita M, Gupta AK, Katsuki M, Kishimoto H, Hasegawa T, High Temperature Air Combustion: From Energy Conservation to Pollution Reduction, CRC Press LLC, 2003.
[2] Cavaliere A, de Joannon M, Prog. Energy Combust. Sci. 30 (2004) 329–366.
[3] Dally BB Riesmeier E, Peters N, Combust. Flame 137 (2004) 418–431.
[4] Dally BB, Karpetis AN, Barlow RS, Proc. Combust. Inst 29 (2002) 1147–1154
[5] Medwell PR, Kalt, PAM, Dally, BB, Combust. Flame 148 (2007) 48–61.
[6] Szegö GG, Dally BB, Nathan GJ, Combust. Flame, 156 (2) (2009) 429-438
[7] Pitts WM, Exp Fluids 11 (1991) 125-134.
[8] Pitts WM, Exp Fluids 11 (1991) 135-141.
[9] England G, Kalt PAM, Nathan GJ, Kelso RM., Exp Fluids 48 (2010) 69–80.
[10] Amielh M, Djeridane T, Anselmet F, Fulachier L, Int J Heat Mass Transf 39 (10) (1996) 2149–2164.
[11] Ruffin E, Schiestel R, Anselmet F, Amielh M, Fulachier L, Phys Fluids 6(8) (1994) 2785–2799.
[12] Dimotakis P, Annu. Rev. Fluid Mech. 37 (2005) 329–56.
[13] Takagi T, Shin H, Ishio A, Combust. Flame 37 (1980) 163-170.
[14] Takagi T, Shin H, Ishio A, Combust. Flame 40 (1981) 121-140.
[15] Clements NT, Paul PH, Combust. Flame 102 (1995) 271-284.
[16] Dunn MJ, 'Finite-Rate Chemistry Effects in Turbulent Premixed Combustion', The University of Sydney, Australia, 2008, PhD Thesis.
[17] Medwell PR, Kalt PAM, Dally BB, Combust. Sci. Tech, 181(7) (2009) 937-953.
[18] Chen YC, Kalt PAM, Masri AR, Bilger RW, 2nd Australian Conference on Laser Diagnostics and Fluid Mechanics in Combustion, Monash University Melbourne, Melbourne, 1999, pp. 57-61.